Activation of NMDA receptors promotes dendritic spine development through MMP-mediated ICAM-5 cleavage

Li Tian,[1] Michael Stefanidakis,[1] Lin Ning,[1] Philippe Van Lint,[3] Henrietta Nyman-Huttunen,[1] Claude Libert,[3] Shigeyoshi Itohara,[4] Masayoshi Mishina,[5] Heikki Rauvala,[2] and Carl G. Gahmberg[1]

[1]Division of Biochemistry, Department of Biological and Environmental Sciences, Faculty of Biosciences, and [2]Neuroscience Center, University of Helsinki, FIN-00014 Helsinki, Finland
[3]Department for Molecular Biomedical Research, Flanders Interuniversity Institute for Biotechnology and Ghent University, B-9052 Ghent (Zwijnaarde), Belgium
[4]Laboratory of Behavioral Genetics, Institute of Physical and Chemical Research, Brain Science Institute, Wako, 351-0198, Japan
[5]Department of Molecular Neurobiology and Pharmacology, Graduate School of Medicine, University of Tokyo, Bunkyo-ku, Tokyo, 113-0033, Japan

Matrix metalloproteinase (MMP)-2 and -9 are pivotal in remodeling many tissues. However, their functions and candidate substrates for brain development are poorly characterized. Intercellular adhesion molecule-5 (ICAM-5; Telencephalin) is a neuronal adhesion molecule that regulates dendritic elongation and spine maturation. We find that ICAM-5 is cleaved from hippocampal neurons when the cells are treated with *N*-methyl-D-aspartic acid (NMDA) or α-amino-3-hydroxy-5-methylisoxazole-propionic acid (AMPA). The cleavage is blocked by MMP-2 and -9 inhibitors and small interfering RNAs. Newborn MMP-2– and MMP-9–deficient mice brains contain more full-length ICAM-5 than wild-type mice. NMDA receptor activation disrupts the actin cytoskeletal association of ICAM-5, which promotes its cleavage. ICAM-5 is mainly located in dendritic filopodia and immature thin spines. MMP inhibitors block the NMDA-induced cleavage of ICAM-5 more efficiently in dendritic shafts than in thin spines. ICAM-5 deficiency causes retraction of thin spine heads in response to NMDA stimulation. Soluble ICAM-5 promotes elongation of dendritic filopodia from wild-type neurons, but not from ICAM-5–deficient neurons. Thus, MMPs are important for ICAM-5–mediated dendritic spine development.

Introduction

Dendritic spines are small, actin-rich protrusions scattered along dendrites, and they carry the postsynaptic components of >90% of excitatory synapses. Despite of being tiny in size, spines are highly dynamic structures that continuously undergo changes in shape and size over time (Hering and Sheng, 2001; Yuste and Bonhoeffer, 2004). A multitude of molecules has been implicated in dendritic spine development and remodeling. Among these, the neurotransmitter receptors, especially *N*-methyl-D-aspartic acid (NMDA) receptor (NR) and α-amino-3-hydroxy-5-methylisoxazole-propionic acid (AMPA) receptor (GluR), which are well-known inducers of spine formation, regulate spine maturation and stabilization via calcium-dependent regulation of filamentous actin turnover (Matus, 2000; Oertner and Matus, 2005). Besides, other cell surface molecules also influence spine properties in response to external signals by mediating cell adhesion and regulating the networks of interconnected signaling pathways, which converge to regulate actin dynamics in spines (Ethell and Pasquale, 2005; Tada and Sheng, 2006).

Cell adhesion molecules (CAMs) and ECM molecules are instrumental in providing physical connections and generating cellular signaling events. Importantly, several recent studies have suggested the involvement of CAMs and ECMs in dendritic spine remodeling (Ethell and Pasquale, 2005) and synaptic plasticity (Washbourne et al., 2004; Gerrow and El-Husseini, 2006). These include N-cadherin (Togashi et al., 2002), syndecan-2

M. Stefanidakis and L. Ning contributed equally to this paper.

Correspondence to Li Tian: li.tian@helsinki.fi

M. Stefanidakis's present address is Department of Pathology, Harvard Medical School, Brigham and Women's Hospital, Center for Excellence in Vascular Biology, Boston, MA 02115.

Abbreviations used in this paper: AMPA, α-amino-3-hydroxy-5-methylisoxazole-propionic acid; CAM, cell adhesion molecule; CTF, C-terminal fragment; DIV, day in vitro; DNQX, 6,7,-dinitroquinoxaline-2,3 (1H,4H)-dione; ICAM, intercellular adhesion molecule; LTP, long-term potentiation; MALDI-TOF, matrix-assisted laser desorption/ionization–time of flight; MAP, microtubule-associated protein; MMP, matrix metalloproteinase; NMDA, *N*-methyl-D-aspartic acid; NR, NMDA receptor; NTF, N-terminal fragment; PSD, postsynaptic density; sICAM-5, soluble ICAM-5; WT, wild type.

The online version of this article contains supplemental material.

The Journal of Cell Biology, Vol. 178, No. 4, August 13, 2007 687–700
http://www.jcb.org/cgi/doi/10.1083/jcb.200612097

(Ethell et al., 2001), neural CAM (Dityatev et al., 2004), integrins (Shi and Ethell, 2006), laminins (Oray et al., 2004), and reelin (Liu et al., 2001).

Intercellular adhesion molecule-5 (ICAM-5; Telencephalin) belongs to the Ig superfamily (Yoshihara et al., 1994; Gahmberg et al., 1998). It is specifically expressed in the postnatal excitatory neuronal cell bodies, dendritic shafts, and dendritic filopodia of the telencephalon (Benson et al., 1998; Mitsui et al., 2005). The expression of ICAM-5 temporally parallels dendritogenesis and synaptogenesis (Yoshihara et al., 1994). In agreement, ICAM-5 has been shown to promote dendritic elongation and branching of hippocampal neurons in vitro (Tian et al., 2000). ICAM-5–deficient mice exhibited decreased density of dendritic filopodia, accelerated maturation of dendritic spines (Matsuno et al., 2006), and changes in long-term potentiation (LTP) in the hippocampus (Nakamura et al., 2001).

Soluble ICAM-5 (sICAM-5) has been detected in physiological fluids under several pathological conditions (Guo et al., 2000; Lindsberg et al., 2002; Borusiak et al., 2005). However, the nature of candidate proteinases and the physiological meaning of the proteolytic cleavage of membrane-bound ICAM-5 have remained unknown.

Matrix metalloproteinases (MMPs) form a large family of mostly secreted, zinc-dependent endopeptidases, which are important for the regulation of cellular behavior through proteolytic cleavage of ECMs and cell surface proteins (Malemud, 2006). Although a large body of data has connected MMPs to brain injury and pathology, accumulating evidence has extended their roles into the normal physiological functions of the brain (Dzwonek et al., 2004; Luo, 2005; Ethell and Ethell, 2007).

Among MMPs, MMP-2 and -9 are most abundantly expressed in the developing brain. MMP-2 is found mainly in astrocytes, whereas MMP-9 is highly expressed in neuronal cell bodies and dendrites (Szklarczyk et al., 2002; Ayoub et al., 2005). The expression and activity of MMP-9 have been shown to depend on NR activation and LTP (Meighan et al., 2006; Nagy et al., 2006). Growing data also suggest the association of MMP-9 (Meighan et al., 2006; Nagy et al., 2006) and other ECM-degrading enzymes (Oray et al., 2004; Bilousova et al., 2006; Monea et al., 2006) with dendritic spine remodeling, synaptic plasticity, learning, and memory formation. Although several ECMs and cell surface proteins, which play important roles in the aforementioned functions, have been identified as MMP substrates, the target molecules for MMP-2 or -9 in the brain have remained largely elusive.

In the present study, we examined the possibility of ICAM-5 acting as a substrate for MMP-2 or -9, using a variety of experimental approaches, and investigated the role of MMP-mediated ICAM-5 proteolytic cleavage in the regulation of dendritic spine development.

Results

NMDA and AMPA promote cleavage of ICAM-5 from hippocampal neurons

Because sICAM-5 has been detected under various pathological conditions, we studied whether ICAM-5 cleavage takes place during physiological neuronal maturation. For this purpose, we examined the release of sICAM-5 from cultured hippocampal neurons at different developmental stages in vitro (3–21 d in vitro [DIV]). The expression of full-length ICAM-5 of 130 kD was low in the 3-DIV hippocampal neurons, but starting from 7 DIV, when dendrites extensively develop in hippocampal neurons, the expression of full-length ICAM-5 dramatically increased and reached a plateau thereafter (Fig. 1, A and B, right). In comparison with this, sICAM-5 of 85–110 kD was most strongly released at 14–21 DIV (Fig. 1, A and B, left), which parallels the period of dendritic spine maturation and synaptic formation. This indicates that the cleavage of membrane-bound ICAM-5 may play an important role during spine maturation.

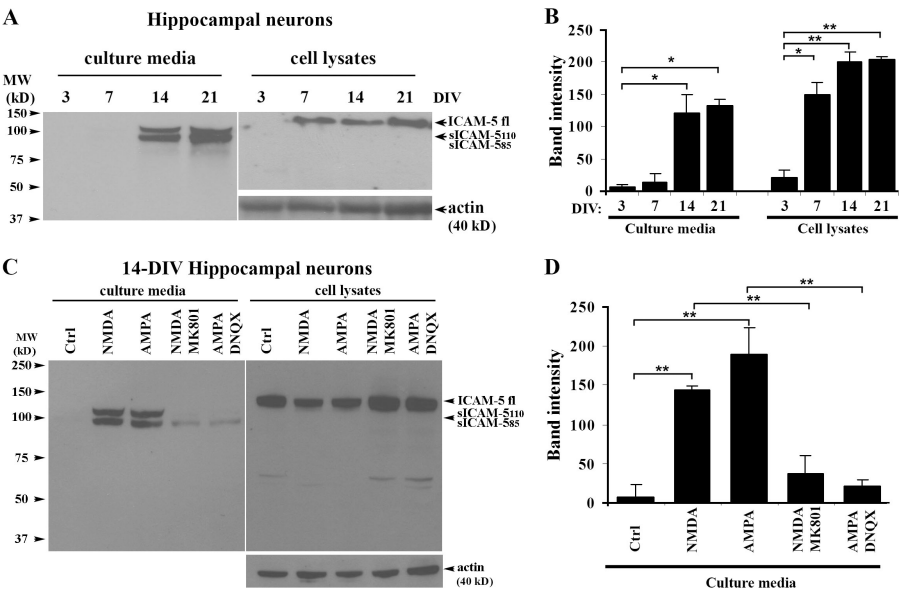

Figure 1. **Cleavage of ICAM-5 from hippocampal neurons is promoted by NMDA and AMPA.** (A) Cell lysates and culture media from rat primary hippocampal neurons of different developmental stages (3–21 DIV) were collected separately, and ICAM-5 was detected by polyclonal antibodies against the ICAM-5 cytoplasmic tail (ICAM-5cp) or ectodomains (1000J), respectively. sICAM-5 of 85- and 110-kD fragments were released into the media and reached a maximum at 14–21 DIV, whereas the expression of full-length ICAM-5 of 130 kD in neurons started to increase from 7 DIV onward. (B) Quantitative analysis of band intensities. (C) In 14-DIV hippocampal neurons, 5 μM NMDA or AMPA treatment caused a significant release of the sICAM-5 fragments with a concomitant reduction of the membrane-bound ICAM-5-fl level, which was inhibited by 20 μM of their respective antagonists, MK801 or DNQX. Half of each medium sample was applied to SDS-PAGE gel for analysis. (D) Quantitative analysis of band intensities of the sICAM-5_{110} from the culture media. Error bars indicate mean ± SD. *, $P < 0.05$; **, $P < 0.01$.

The NRs and GluRs are key regulators of spine formation and maturation. Therefore, we tested the effects of NMDA and AMPA on ICAM-5 cleavage from hippocampal neurons. In 14-DIV hippocampal neurons, 5 μM NMDA or AMPA treatment caused significant release of the sICAM-5 fragments of 110 and 80–85 kD, with concomitant reduction of the membrane-bound ICAM-5 (Fig. 1, C and D). Moreover, the cleavage of ICAM-5 was inhibited by the NMDA antagonist MK801 and the non-NMDA antagonist DNQX (6,7,-dinitroquinoxaline-2,3[1H,4H]-dione; Fig. 1, C and D).

MMP-2 and -9 cleave the membrane-bound ICAM-5

To further investigate the mechanism of ICAM-5 proteolytic cleavage, we used various chemical or peptide inhibitors of MMPs. As shown in Fig. 2, ICAM-5 cleavage was almost completely inhibited by the broad-spectrum MMP inhibitor GM6001, but not by its negative control. A variety of MMP-2 and -9 inhibitors also partially or completely blocked the cleavage (Fig. 2, A and B). These data provide the first evidence that MMP-2 and -9, especially when activated by

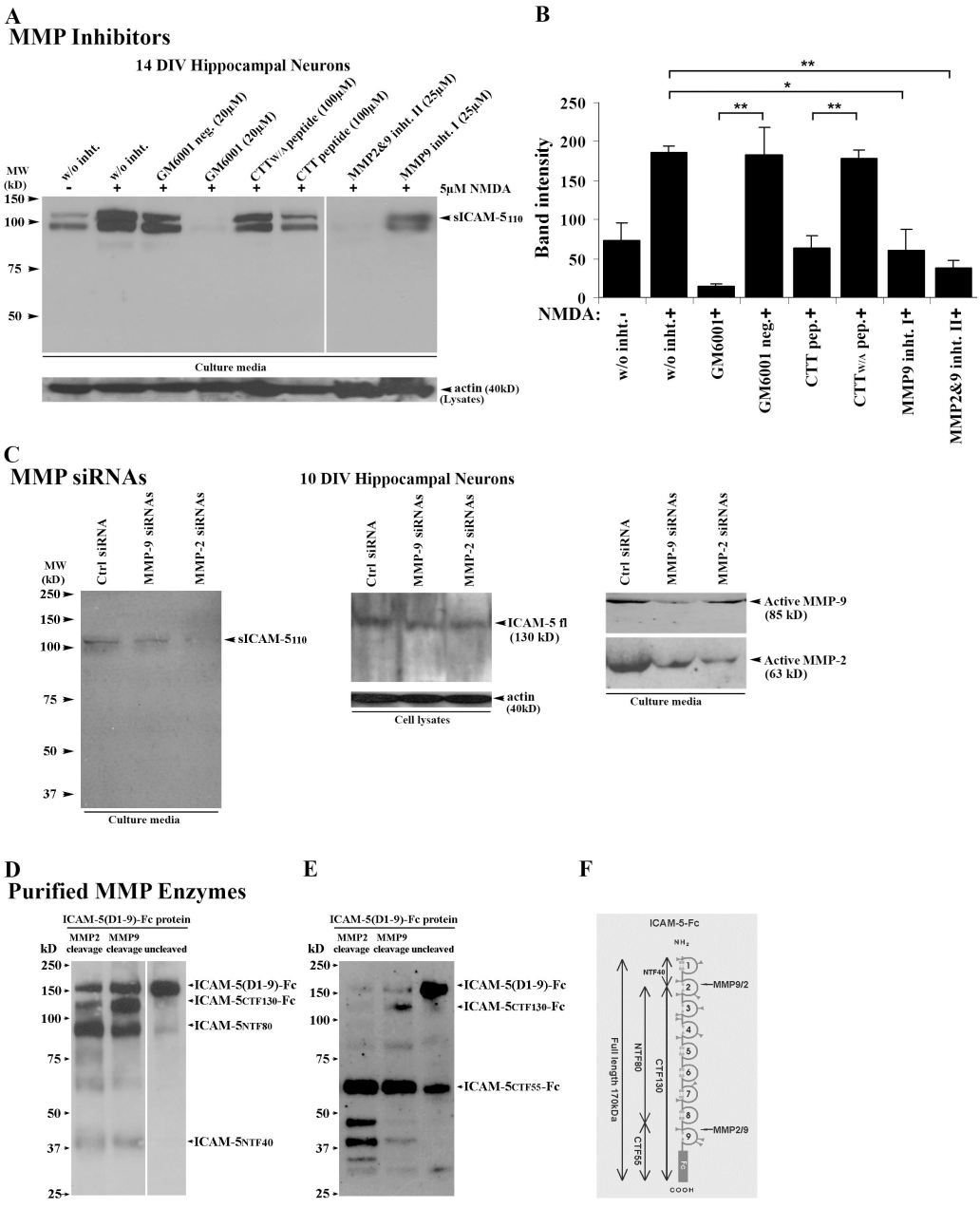

Figure 2. **Cleavage of ICAM-5 is mediated by MMP-2 and -9.** (A) 14-DIV neurons were left untreated or treated with NMDA in the presence of MMP inhibitors. The NMDA-induced cleavage of ICAM-5 was blocked by MMP-2 and -9 inhibitors, as compared with the negative controls. Actin in cell lysates was used to quantitate the amount of cells from which the culture media were collected. (B) Quantitative analysis of A. Error bars indicate mean ± SD. *, $P < 0.05$; **, $P < 0.01$. (C) The siRNAs for rat MMP-2 and -9 transfected into the 9-DIV neurons efficiently blocked the ICAM-5 cleavage. Incubation of recombinant mouse ICAM-5 D1-9-Fc protein with active MMP-2 or -9 enzyme resulted in cleavage of the recombinant protein into multiple fragments, as detected by anti–ICAM-5 (D) or anti-Fc antibody (E). Interestingly, the two MMPs seemed to prefer different cleavage sites, although both cleave ICAM-5 in a similar way, as depicted in F. The indicated cleaved fragments (CTF130, NTF80, and NTF40) were analyzed by mass spectrometry peptide mapping.

NMDA, are mainly responsible for the proteolytic cleavage of ICAM-5.

Because the expression and activity of MMP-9 have been shown to be up-regulated in response to stimuli that induce NR activation and LTP (Meighan et al., 2006; Nagy et al., 2006), we tested the conditioned culture media from treated hippocampal neurons and found increased levels of both active MMP-2 and -9 upon NMDA stimulation (Fig. S1, available at http://www.jcb.org/cgi/content/full/jcb.200612097/DC1). We then used the RNA interference technique to temporarily decrease the expression of MMP-2 or -9 in hippocampal neurons (Fig. 2 C). After transfection into neurons, the MMP-2 and -9 siRNAs substantially decreased the protein levels of MMP-2 and -9, respectively (Fig. 2 C, right), with the concomitant inhibition of ICAM-5 cleavage from the transfected neurons (Fig. 2 C, left).

We further incubated the recombinant mouse ICAM-5 D1-9-Fc protein with activated MMP-2 or -9 and studied the cleavage using anti–ICAM-5 polyclonal antibody 1000J (Fig. 2 D) or anti-Fc polyclonal antibody (Fig. 2 E) in Western blots. The cleaved proteins were then analyzed by matrix-assisted laser desorption/ionization–time of flight (MALDI-TOF) peptide mass mapping to identify the individual fragments (C-terminal fragment [CTF] 130-Fc, N-terminal fragment [NTF] 80–85, and NTF40; Fig. S2, available at http://www.jcb.org/cgi/content/full/jcb.200612097/DC1). We found that both MMP-2 and -9 cut at similar sites in the second and ninth ectodomains of ICAM-5, as depicted in Fig. 2 F. Interestingly, they seemed to show selectivity for the cleavage sites, as shown by the intensities of the fragments they produced. The minor bands detected within 30–75 kD in Fig. 2 (D and E) may be caused by protein degradation.

Dissociation of ICAM-5 from the cytoskeleton promotes its cleavage

Because the NRs and GluRs are known to regulate actin dynamics, we examined whether the NR-promoted cleavage of ICAM-5 is dependent on its anchorage to actin filaments. Interestingly, we found that cytochalasin D and latrunculin A, which prevent actin polymerization by capping the barbed end of actin filaments and monomeric actin, respectively, significantly increased the cleavage of ICAM-5 (Fig. 3, A and B). This indicates that the association between ICAM-5 and actin filaments may affect the MMP-mediated proteolytic cleavage. Furthermore, we found that treatment of hippocampal neurons with 20 μM NMDA for 1 h resulted in a considerable release of ICAM-5 from the cytoskeletal fraction into the soluble fraction of neuronal lysates (Fig. 3, C and D). These findings strongly support the hypothesis that dissociation of ICAM-5 from the actin cytoskeleton promotes its cleavage.

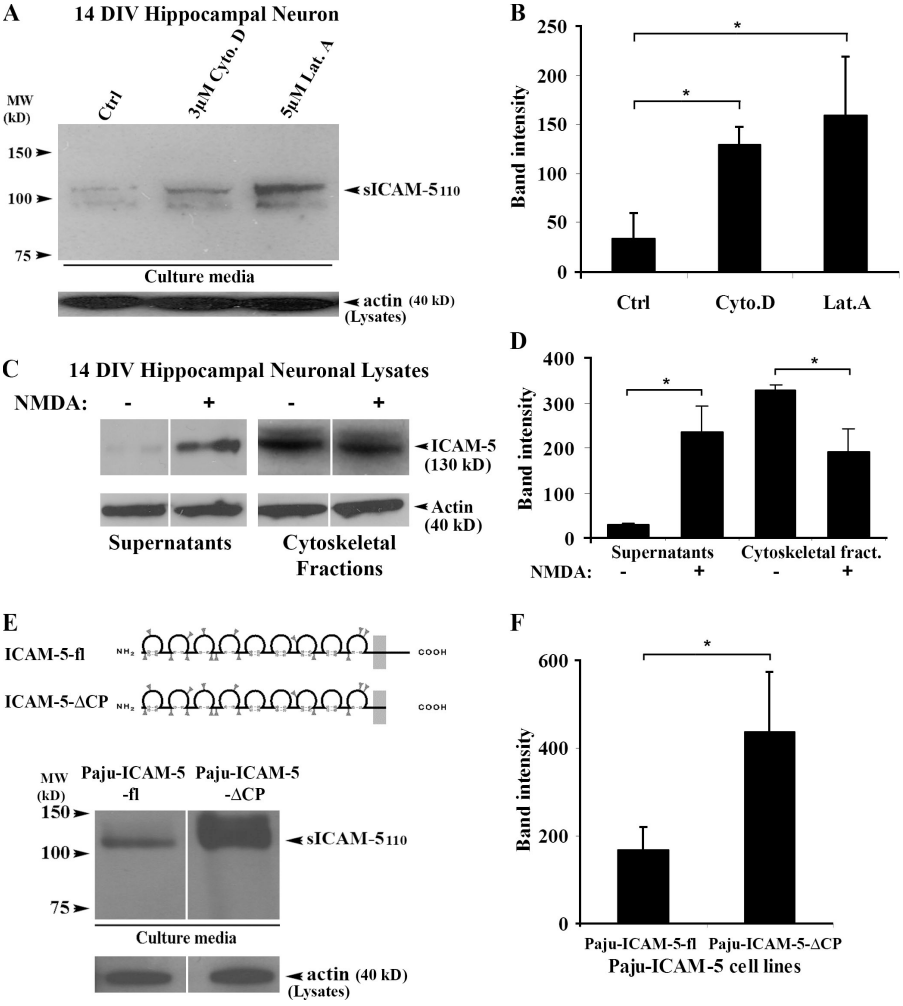

Figure 3. **Dissociation of ICAM-5 from the actin cytoskeleton promotes its cleavage.** 14-DIV neurons were left untreated or treated with cytochalasin D or latrunculin A. The results from Western blotting (A) and quantitative analysis of the band intensities (B) showed that both cytochalasin D and latrunculin A strongly increased the cleavage of ICAM-5. Furthermore, 14-DIV neurons were treated with 20 μM NMDA for 60 min before being lysed, and the lysates were then separated by ultracentrifugation into soluble fractions, which contain dissolved membrane proteins and soluble cytosolic proteins, and cytoskeletal fractions, which contain the majority of actin filaments. Detection of ICAM-5 and actin showed dissociation of ICAM-5 from the actin cytoskeleton after NMDA treatment (C). (D) ICAM-5 levels in the soluble and cytoskeletal fractions were quantified. Moreover, the transfected neural crest cell lines, Paju-ICAM-5-fl and Paju-ICAM-5-ΔCP, which expressed full-length or cytoplasmic tail-truncated ICAM-5, respectively, were analyzed (E and F). Schematic drawings of the two ICAM-5 constructs are shown. Paju-ICAM-5-ΔCP cells released a considerably larger amount of the sICAM-5 than Paju-ICAM-5-fl cells (E and F). Quantitation of actin was done as described in Fig. 2 A. Error bars indicate mean ± SD. *, $P < 0.05$.

To further study this phenomenon, we compared Paju-ICAM-5-fl and Paju-ICAM-5-ΔCP cell lines, which express the full-length ICAM-5 or the truncated ICAM-5 without the cytoplasmic domain (Fig. 3 E), respectively. We have shown that truncation of the cytoplasmic tail of ICAM-5 results in a more diffuse distribution of the molecule on the plasma membrane and reduced colocalization with the subcortical actin filaments (Nyman-Huttunen et al., 2006). The cell surface expression level of ICAM-5 on both cell lines was comparable (Fig. S3, available at http://www.jcb.org/cgi/content/full/jcb.200612097/DC1). Compared with Paju-ICAM-5-fl, Paju-ICAM-5-ΔCP cells showed a considerable increase of ICAM-5 cleavage (Fig. 3, E and F).

Abnormal ICAM-5 expression during early postnatal development of MMP-2– and MMP-9–deficient mice

To further clarify the involvement of MMP-2 and -9 on ICAM-5 cleavage, we studied the expression of ICAM-5 in MMP-deficient mice at different postnatal developmental stages (from postnatal 1 d to 10 wk). ICAM-5 expression was increased in all MMP-deficient mice after birth, whereas L1CAM showed a decreased expression (Fig. 4, A and C). Moreover, it is noteworthy that, compared with the wild-type (WT) mice, the MMP-$2^{-/-}$ and MMP-$9^{-/-}$ deficient mice contained significantly more full-length ICAM-5 at the early postnatal stage (postnatal day 1). However, the MMP-$2^{-/-}$/MMP-$9^{-/-}$ double-deficient mice expressed lower levels of ICAM-5 (Fig. 4, A and C). The changes in the MMP-$2^{-/-}$, MMP-$9^{-/-}$, and MMP-$2^{-/-}$/MMP-$9^{-/-}$ double-deficient mice tended to disappear after 1 wk postnatally, except in the MMP-$2^{-/-}$/MMP-$9^{-/-}$ double-deficient mice, where ICAM-5 expression still remained slightly but significantly lower than in the WT mice (Fig. 4, A and C). Studies on the enzymatic activities of MMP-2 and -9 by gelatinase zymography verified the identity of the respective deficient mice (Fig. 4 B) and indicated that the activity of MMP-2 in both the MMP-$9^{-/-}$ deficient mice and the WT mice decreased during the postnatal development. However, there seemed to be some compensating up-regulation of the proMMP-9 level in the adult MMP-$2^{-/-}$

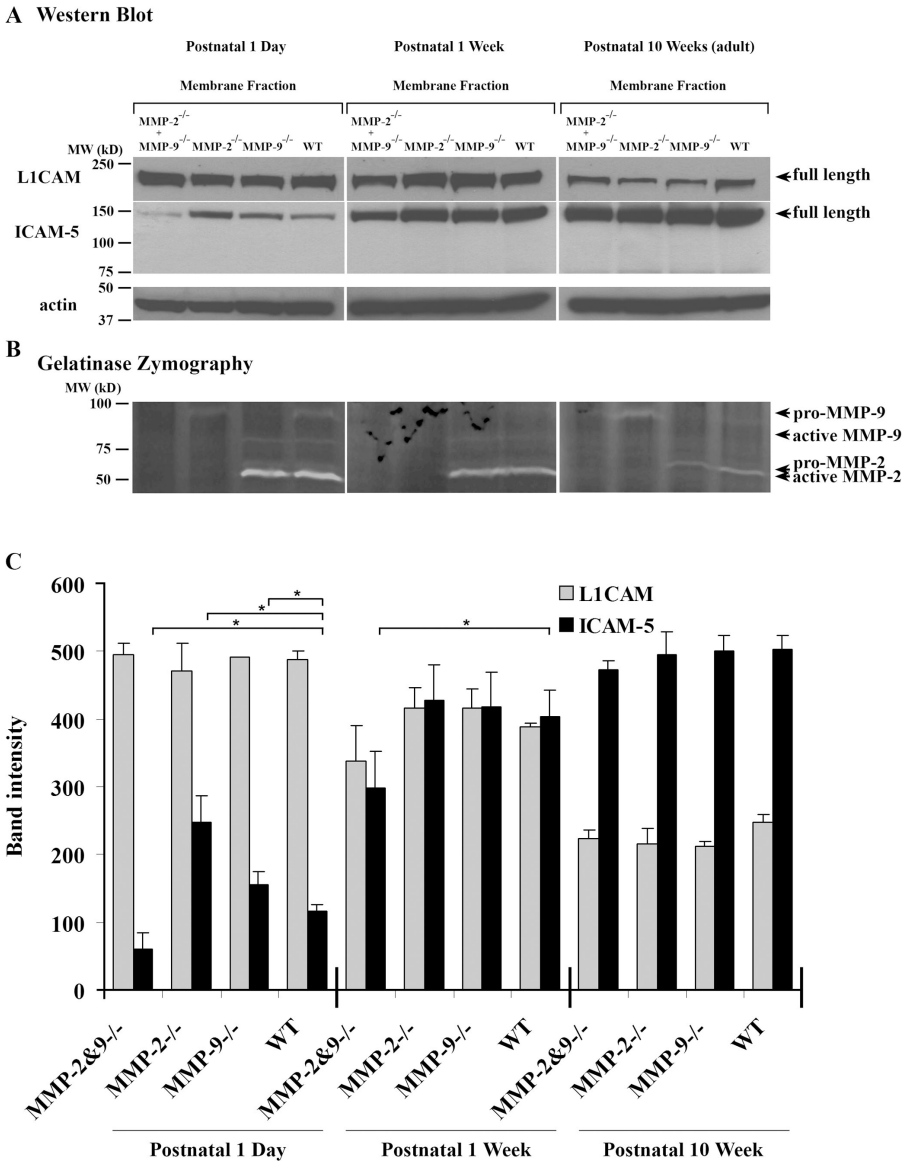

Figure 4. **ICAM-5 expression is abnormal during early postnatal development of MMP-2– and MMP-9–deficient mice.** The forebrains from postnatal (1 d to 10 wk) MMP-deficient and WT mice were homogenized, and the membrane fractions were obtained by ultracentrifugation. The results from Western blotting (A) and quantitative analysis of the band intensities (C) both showed that in postnatal 1-d mice, the expression levels of ICAM-5 were significantly higher in MMP-$2^{-/-}$ and MMP-$9^{-/-}$ mice than in WT mice, whereas in MMP-$2^{-/-}$/MMP-$9^{-/-}$ double-deficient mice, the expression was lower (A and C, left). Error bars indicate mean ± SD. *, $P < 0.05$. After the first postnatal week, ICAM-5 expression was increased in all mice, and the difference was not as obvious as before, although a considerably lower amount was still detected in the double-deficient mice (A and C, middle and right). In comparison, the expression of L1CAM gradually decreased during the postnatal period, and little difference between the deficient and WT mice was observed. *, $P < 0.05$. (B) Gelatinase zymography confirmed the identity of each type of mice and showed that the activity of MMP-2 considerably decreased during the postnatal development of the brain.

deficient mice, which was not obvious in the younger mice (Fig. 4 B, right). Similar findings have been reported (Esparza et al., 2004).

Our histological analysis of the brains of MMP-2– and MMP-9–deficient mice showed that both, especially the MMP-2–deficient mice, had abnormal cerebral cortical and hippocampal structures. The cortical layers 2–3 seemed to have increased number of cells (Fig. S4, available at http://www.jcb.org/cgi/content/full/jcb.200612097/DC1). Similar findings have been reported in the cerebellar cortex of MMP-9–deficient mice, which showed an abnormal accumulation of granular precursors in the external granular layer (Vaillant et al., 2003). We believe that the increased level of ICAM-5 in MMP-2–deficient mice is not due to the increased number of neurons in the cortex, because we carefully controlled the protein load per sample and monitored the amount of loaded actin during Western blotting.

ICAM-5 is enriched in filopodia and thin spines but not in mature mushroom spines

Dendritic spines occur in a range of sizes and in a variety of shapes, commonly classified as thin, stubby, and mushroom (Hering and Sheng, 2001; Yuste and Bonhoeffer, 2004). There is a strong correlation between the size of the spine head and the strength of the synapse, presumably related to the higher levels of GluRs in larger spines (Kasai et al., 2003). There is also evidence that the smaller weaker spines preferentially undergo LTP, whereas larger spines are more stable and show less plasticity (Matsuzaki et al., 2004). Such observations have led to the view that thin spines represent "plasticity spines" and large mushrooms "memory" spines (Kasai et al., 2003).

ICAM-5 was earlier found to be mainly expressed in dendritic filopodia, and its expression inversely correlated with synapse maturation (Matsuno et al., 2006). To further clarify whether ICAM-5 is distinctively expressed in spines at different maturation stages, we studied the dendritic protrusions of 10–17-DIV hippocampal neurons. Such neurons contain various dendritic protrusions, including filopodia, small-head thin spines, and large-head mushroom spines. The dendritic fine structures were visualized by transfection of the EGFP into the 12-DIV neurons. The overlapping of immunostained ICAM-5 with EGFP was measured by calculation of the Pearson's colocalization efficiency (Fig. 5). Our result showed that ICAM-5 was more abundantly expressed in filopodia (Fig. 5 A, arrow) and thin spines (Fig. 5 A, arrowheads) but much less in the mushroom spines (Fig. 5 A, asterisks), particularly when the heads of the two different types of spines were compared (Fig. 5 A). These data suggest that ICAM-5 may play a more active role in the "plastic" thin spines than in the more "stable" mushroom spines.

Activation of the NRs decreases the colocalization of ICAM-5 with F-actin

Because we found that activation of the NRs led to dissociation of membrane-bound ICAM-5 from the actin cytoskeleton, it became important to study ICAM-5 and F-actin distributions in neurons upon activation of NRs. We treated the 10-DIV hippocampal neurons with 5 μM NMDA and triple stained the neurons for the ICAM-5 cytoplasmic tail, the F-actin, and the postsynaptic density (PSD) 95 protein (Fig. 6 A). Treatment of hippocampal neurons with NMDA resulted in reduced colocalization of ICAM-5 with F-actin not only along dendritic shafts (Fig. 6, A and B) but also in thin and mushroom spines (Fig. 6 A, arrowheads and asterisks, respectively). The reduced colocalization of ICAM-5 with F-actin was partially counteracted by pretreatment of neurons with the NR antagonist MK801 (Fig. 6, A and B). NMDA treatment led to a significantly increased amount of mushroom spines (Fig. 6 C).

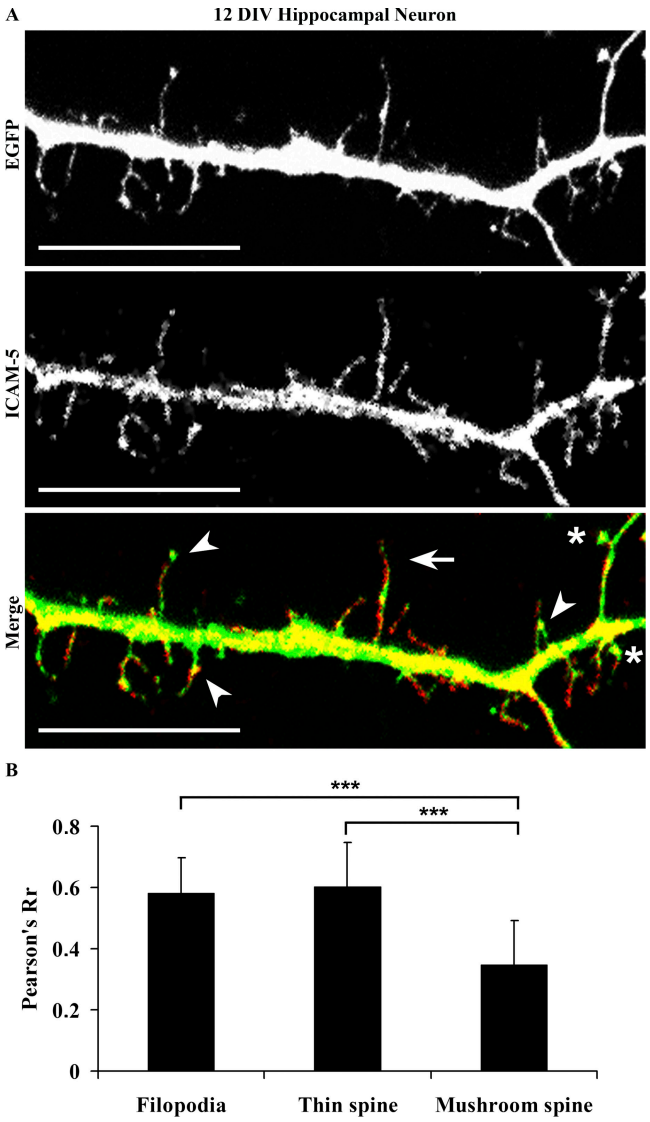

Figure 5. **ICAM-5 is enriched in thin spines rather than in mushroom spines.** (A) 12-DIV hippocampal neurons were transfected with EGFP and immunostained with anti–ICAM-5cp polyclonal antibody. ICAM-5 was strongly expressed in dendritic shafts. In the protrusions along the shaft, ICAM-5 was clearly located in filopodia (arrow) and thin spines (arrowheads), but much less in mushroom spines (asterisks), especially when the heads of the two different types of spines were compared (A). The colocalization of ICAM-5 with EGFP in different protrusions was analyzed and represented by Pearson's coefficiency (Rr). Mushroom spines gave the least colocalization degree, whereas thin spines and filopodia gave higher values (B). Error bars indicate mean ± SD. ***, $P < 0.001$. Bars, 10 μm.

The NR-induced cleavage of ICAM-5 is blocked by MMP inhibitors along dendritic shafts but not in thin spines

Because we found that NMDA and AMPA reduced anchorage of ICAM-5 to the actin cytoskeleton and promoted its cleavage through MMP-2 and -9, these facts could be the reasons for the exclusion of ICAM-5 from maturating spines. Therefore, it was important to study whether the ICAM-5 cleavage from spines, as a result of activation of the NRs, could be blocked by MMP inhibitors. For this purpose, we studied the EGFP-transfected 17-DIV hippocampal neurons that were treated with 5 μM NMDA and various MMP inhibitors (Fig. 7 A). To measure the effects of MMP inhibitors more accurately, ICAM-5 was visualized by immunostaining with a mAb that recognizes its extracellular region. We found that NMDA reduced the localization of ICAM-5 in both the dendritic shafts and thin spines in 17-DIV neurons (Fig. 7 A), similar to what was observed in younger neurons (Fig. 6). Blocking the NRs with MK801 clearly recovered the localization of ICAM-5 in both shafts and thin spines. When various MMP inhibitors, including the general inhibitor GM6001, the MMP-2/9–specific peptide inhibitor CTT, and the inhibitor II, were applied together with NMDA, most ICAM-5 along dendritic shafts was recovered (Fig. 7 A). However, the recovery of ICAM-5 in thin spines, especially in spine heads, was much less efficient by inhibition of MMPs, as compared with the NR antagonist MK801 (Fig. 7, A and B). This may be due to the fact that ICAM-5 was more vulnerable for MMPs in spine heads, which contain highly motile and dynamic actin filaments, as compared with the shafts that contain a more stable actin cytoskeleton. We further found that pretreatment with the MMP-2/9 inhibitor II significantly decreased the number of spines induced by NMDA (Fig. 7 C).

WT and ICAM-5–deficient neurons respond differently to NMDA stimulation

To further study the function of ICAM-5 in thin spines, we compared the response of WT and ICAM-5$^{-/-}$ hippocampal neurons to NMDA stimulation. The EGFP-transfected 17-DIV fixed neurons were first immunostained for ICAM-5 and PSD95. ICAM-5 immunostaining verified the identity of ICAM-5$^{-/-}$ neurons (Fig. 8 A). In addition, the size of mushroom spines in ICAM-5$^{-/-}$ neurons seemed to be larger than those in WT neurons,

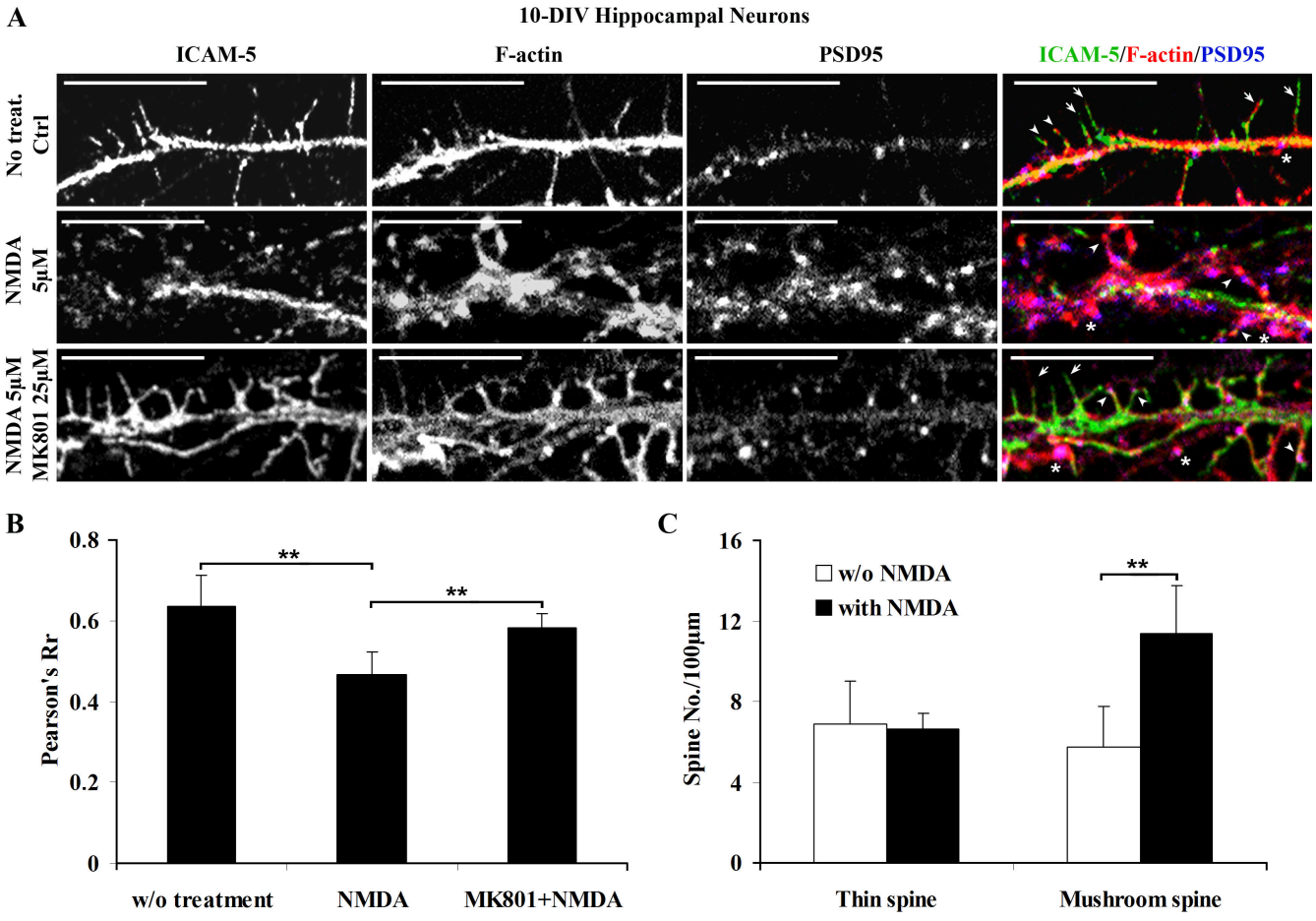

Figure 6. **NMDA decreases the colocalization of ICAM-5 with F-actin in spines.** (A) 10-DIV hippocampal neurons were left untreated or treated for 6 h with 5 μM NMDA, with or without a 1-h pretreatment with the NR antagonist MK801. The neurons were then triple stained for ICAM-5 (green), F-actin (red), and PSD95 (blue). ICAM-5 colocalized with F-actin in dendritic filopodia (arrows) and thin spines (arrowheads), but much less in mushroom spines (asterisks). (B) The degree of colocalization between ICAM-5 and F-actin was analyzed after the above treatments. Note that NMDA significantly decreased the colocalization of ICAM-5 with F-actin, which was partially counteracted by MK801. (C) The effects of NMDA on formation of thin and mushroom spines were quantified. Error bars indicate mean ± SD. **, $P < 0.01$. Bars, 10 μm.

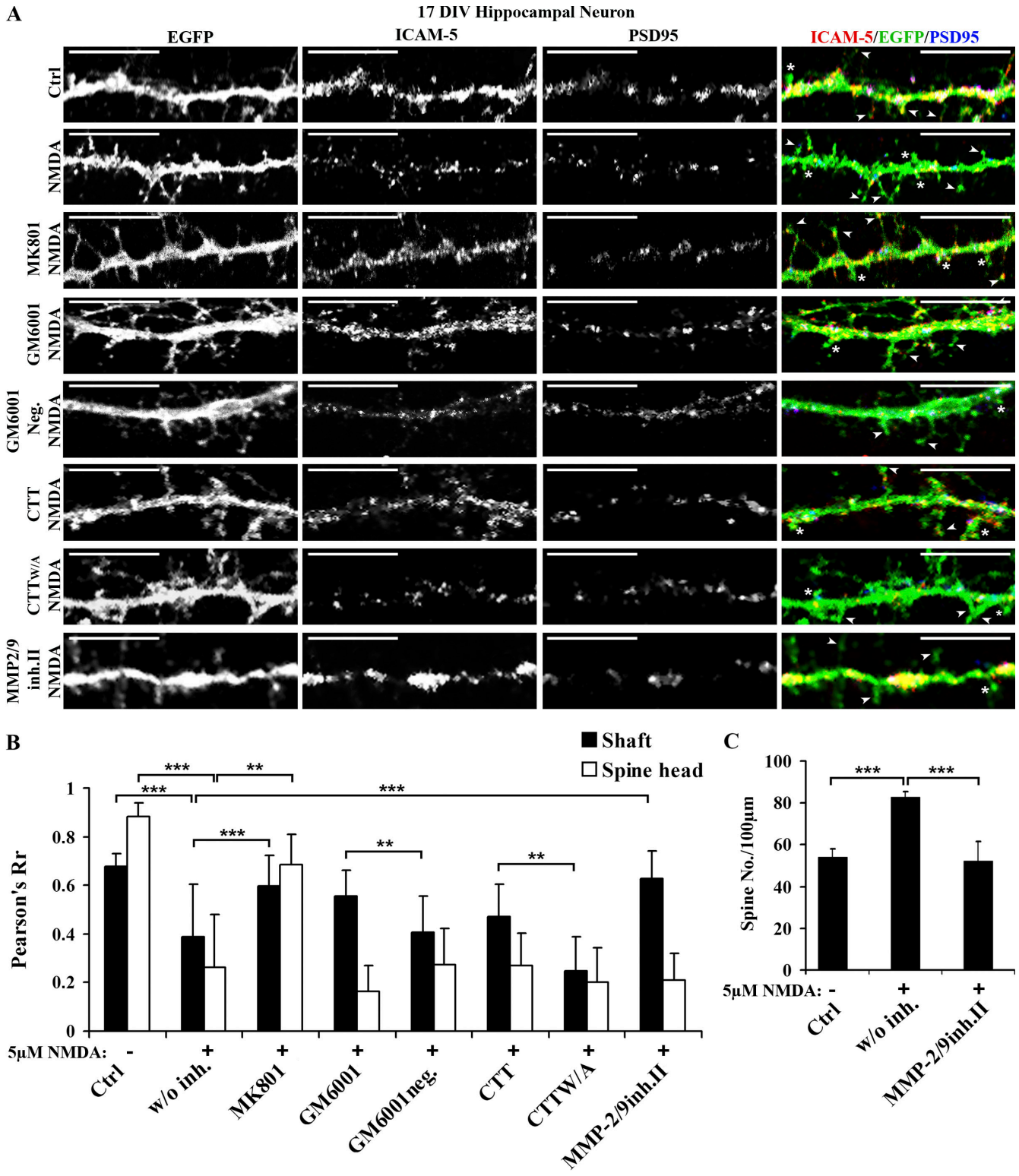

Figure 7. **MMP inhibitors prevent the NMDA-induced ICAM-5 cleavage in dendritic shafts but not in spines.** (A) 17-DIV hippocampal neurons were transfected with EGFP and either left untreated or treated for 6 h with 5 μM NMDA, with or without a 1-h pretreatment with 20 μM MK801 or MMP inhibitors. The neurons were then double stained for ICAM-5 by a mAb against the ectodomains of rat ICAM-5 (red) and PSD95 (blue). (B) The colocalization of ICAM-5 with EGFP in dendritic shafts or thin spine heads was measured. The localization of ICAM-5 in both dendritic shafts and thin spine heads (A, arrowheads) were significantly reduced by NMDA, which was efficiently counteracted by MK801. The MMP broad-spectrum inhibitor GM6001, in comparson to its negative control compound, significantly blocked the NMDA-induced reduction of ICAM-5 localization in dendritic shafts. Similar effects were found with the MMP-2/9–specific inhibitors, CTT peptide, and MMP-2/9 inhibitor II. However, none of the MMP inhibitors gave substantial recovery of ICAM-5 in thin spine heads. Furthermore, MMP-2/9 inhibitor II significantly blocked the NMDA-induced formation of spines (C). The experiment was repeated three times with similar results. Error bars indicate mean ± SD. **, $P < 0.01$; ***, $P < 0.001$. Bars, 10 μm.

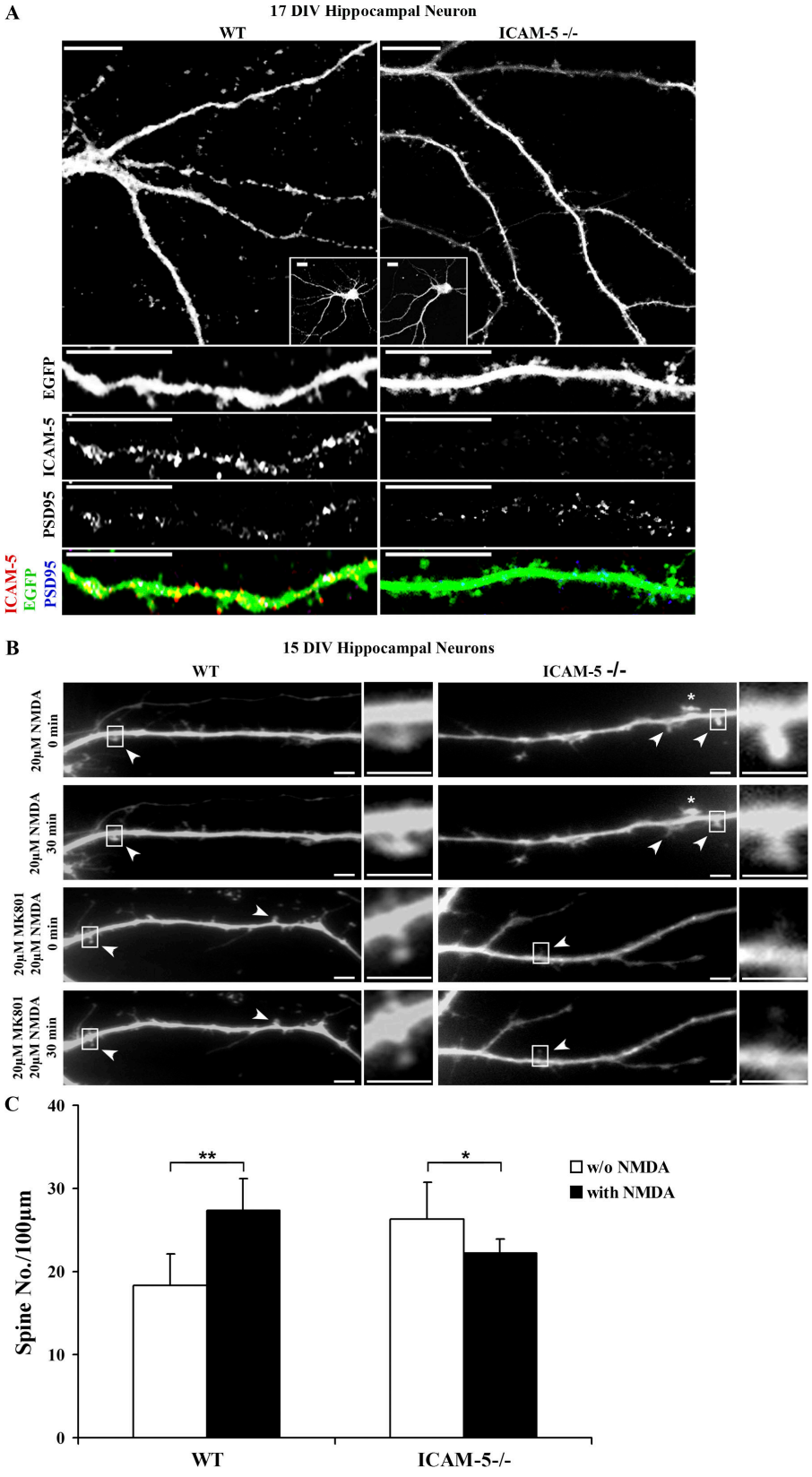

Figure 8. **ICAM-5 deficiency results in retraction of spine heads in response to NMDA stimulation.** (A) The responses of WT and ICAM-5$^{-/-}$ hippocampal neurons to NMDA stimulation were compared. To verify the identity of ICAM-5–deficient neurons, the EGFP-transfected 17-DIV fixed neurons of the two types were immunostained for ICAM-5 and PSD95. The size of mushroom spines in ICAM-5$^{-/-}$ neurons seemed to be larger than those in WT neurons. (B) The 15-DIV EGFP-transfected neurons were then monitored with a time-lapse fluorescence microscope. The neurons were treated by 20 μM NMDA for 1 h with or without a 1-h pretreatment with 20 μM MK801 and recorded during the 1-h period of NMDA stimulation. Thin spines of WT neurons showed increased growth of spine heads in response to NMDA stimulation within 1 h. In contrast, spine heads in ICAM-5$^{-/-}$ neurons seemed to be retracted during the 1-h treatment of NMDA (B, arrowheads). Intriguingly, mushroom spines in ICAM-5$^{-/-}$ neurons respond positively toward NMDA stimulation, with increased size of spine heads (B, asterisks). (C) Spine numbers were increased in WT neurons but not in ICAM-5$^{-/-}$ neurons after treatment with 5 μM NMDA for 8 h. The experiment was repeated three times with similar results. Error bars indicate mean ± SD. *, $P < 0.05$; **, $P < 0.01$. Bars, 3 μm.

which was similar to an earlier report (Matsuno et al., 2006). To monitor the growth of thin spines in these neurons, we studied the 15-DIV EGFP-transfected neurons with a time-lapse fluorescence microscope. The neurons were treated with 20 μM NMDA for 1 h with or without a 1-h pretreatment with MK801, and monitored for 1 h. We found that thin spines in WT neurons showed increased growth of spine heads in response to NMDA stimulation. In contrast, spine heads in ICAM-5$^{-/-}$ neurons seemed to be retracting (Fig. 8 B, arrowheads). Spine numbers were increased in WT neurons, but not in ICAM-5$^{-/-}$ neurons

after treatment with 5 μM NMDA for 8 h (Fig. 8 C). These data indicate that ICAM-5 is important for the motility of thin spines. Interestingly, we also found that mushroom spines in ICAM-5$^{-/-}$ neurons respond positively toward NMDA stimulation, with increased size of spine heads (Fig. 8 B, asterisks).

sICAM-5 promotes dendritic filopodia elongation

To study functions of the sICAM-5, we cultured the EGFP-transfected 9-DIV WT and ICAM-5$^{-/-}$ neurons in the presence of 10 μg/ml recombinant sICAM-5 D1-4-Fc protein for 3 d. The neurons were then immunostained for ICAM-5 and microtubule-associated protein-2 (MAP-2; Fig. 9 A). sICAM-5 D1-4-Fc protein induced a significantly higher number of filopodia from the WT neurons, compared with the ICAM-5$^{-/-}$ neurons (Fig. 9, B and C). The filopodial length of WT neurons also significantly increased in the presence of sICAM-5 D1-4-Fc protein, as compared with the ICAM-5$^{-/-}$ neurons (Fig. 9 D).

Discussion

ICAM-5 has been shown to be gradually excluded from mature synapses, but the mechanism was not elucidated (Matsuno et al., 2006). Here, we show that activation of the NRs induced cleavage of ICAM-5 (Fig. 1), which evidently is mediated by active MMP-2 and -9 (Fig. 2). The association of ICAM-5 with the actin cytoskeleton was decreased in dendritic spines in response to activation of the NRs, which affected the ICAM-5 cleavage (Figs. 3 and 6). ICAM-5 deficiency led to the retraction of spine heads and a decreased number of spines in response to NMDA stimulation (Fig. 8). sICAM-5 protein increased the number and length of filopodia in WT neurons but not in ICAM-5–deficient neurons (Fig. 9).

Combining these data with the earlier findings on ICAM-5 (Tian et al., 2000; Matsuno et al., 2006; Nyman-Huttunen et al., 2006), we present a schematic model depicting the NR-mediated spine development in which ICAM-5 is involved (Fig. 10). NMDA or AMPA stimulation causes increased MMP-2 and -9 activities in neurons and neighboring glial cells (not depicted), resulting in cleavage of the ectodomains of ICAM-5 from immature nascent spines. The reduced membrane level of ICAM-5 may facilitate local membrane and cytoskeleton reorganization, and thereby morphological remodeling of dendritic spines.

We have shown that ICAM-5 promotes dendritic elongation through homophilic interaction (Tian et al., 2000). Our current data further indicate that the increased number and length of filopodia from WT neurons is mediated by the homophilic interaction of sICAM-5 D1-4-Fc protein with membrane-bound

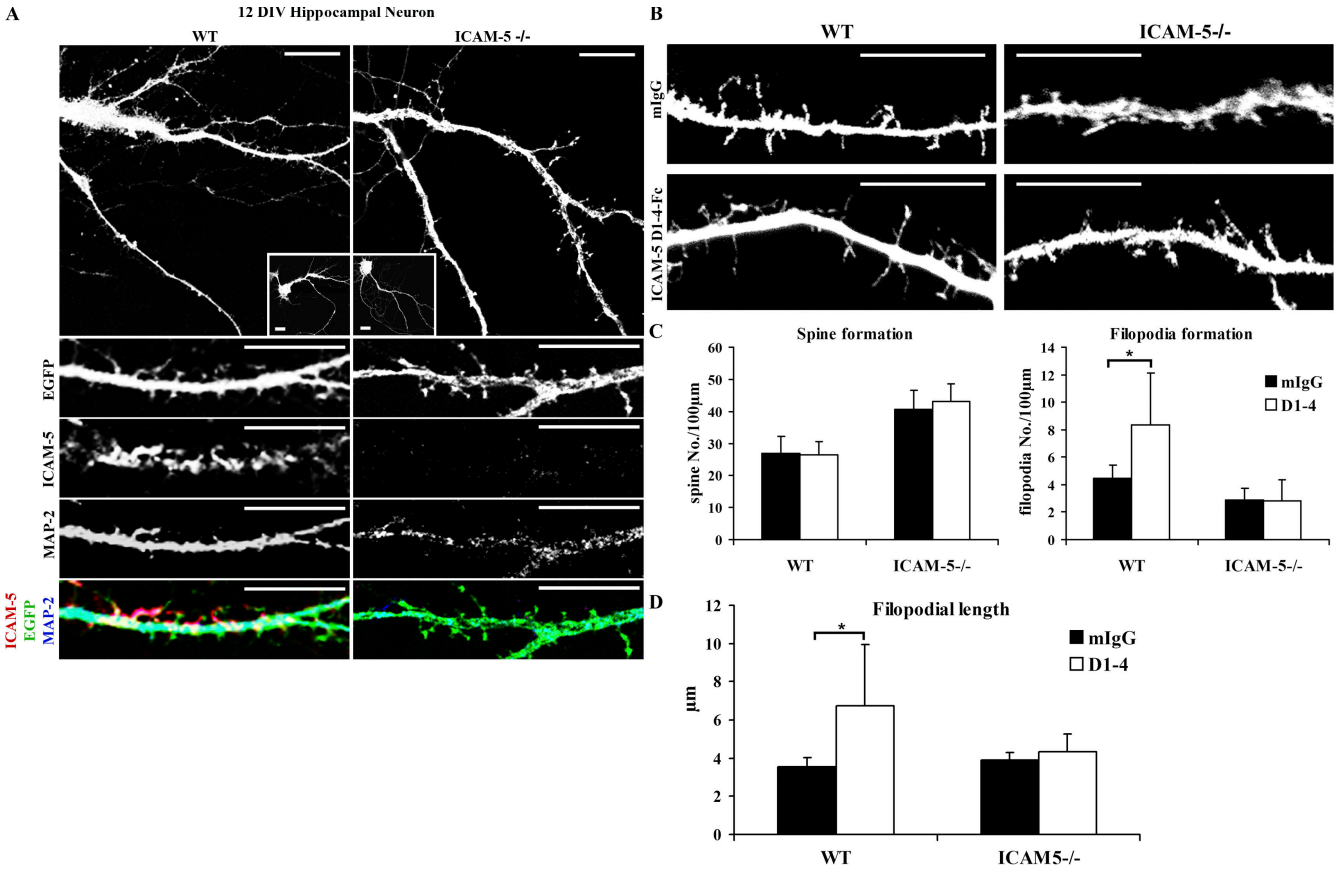

Figure 9. **sICAM-5 promotes dendritic filopodia elongation.** 9-DIV EGFP-transfected WT and ICAM-5$^{-/-}$ hippocampal neurons were incubated with 10 μg/ml soluble recombinant ICAM-5 D1-4-Fc protein or control mIgG for 72 h. The neurons were then double stained for ICAM-5 (A, red) and MAP-2 (A, blue). Compared with mIgG control protein, sICAM-5 D1-4-Fc protein induced significantly more filopodia from WT neurons, but not from ICAM-5$^{-/-}$ neurons (B and C). The filopodial length of WT neurons, but not ICAM-5$^{-/-}$ neurons, also significantly increased in the presence of sICAM-5 D1-4-Fc protein (D). The experiment was repeated three times with similar results. Error bars indicate mean ± SD. *, $P < 0.05$. Bar, 10 μm.

ICAM-5. These data extend our knowledge on functions of ICAM-5 in the context of the NR-regulated dendritic development. Indeed, blocking the ionotropic glutamate receptors has been demonstrated to result in an ~35% decrease in the density and turnover of shaft filopodia, whereas focal glutamate application leads to a 75% increase in the length of shaft filopodia (Portera-Cailliau et al., 2003).

ICAM-5 has been postulated to be a negative regulator of filopodia-to-spine transition (Matsuno et al., 2006). In this sense, the promoted cleavage by NRs implies an important mechanism for a transformation of immature spines toward maturation. Moreover, the cooperative performance of ICAM-5 together with the NRs and MMPs may fine-tune the process of spine remodeling. The phenomenon that thin spines in ICAM-$5^{-/-}$ neurons retracted in response to NMDA treatment (Fig. 8) seems to be contradictory to the fact that ICAM-$5^{-/-}$ neurons have eventually larger mature spines (Matsuno et al., 2006). As the expression of ICAM-5 is the lowest in mature spines, we suspect that the eventual increase in size of mature spine heads is either not directly ICAM-5 related or resulted from secondary effects of ICAM-5 deficiency, which needs further clarification.

We provide several lines of evidence that MMP-2 and -9 are responsible for the proteolytic processing of ICAM-5, leading to the production of the sICAM-5. First of all, we detected a steady-state cleavage of ICAM-5 from the cultured primary neurons, which was increased by NMDA or AMPA stimulation (Fig. 1). As earlier shown, MMP-9 gene expression is up-regulated in response to extracellular stimuli, like growth factors, cytokines, and neurotransmitters, whereas there is lack of transcriptional regulation of MMP-2 expression (Chakraborti et al., 2003; Meighan et al., 2006; Nagy et al., 2006). These facts suggest that MMP-2 is involved in the basal processing of ICAM-5 and MMP-9 in the activity-dependent cleavage of ICAM-5. In addition, NMDA-induced ICAM-5 cleavage was efficiently prevented by various MMP-2 and -9 inhibitors and siRNAs (Fig. 2). Abnormally high expression levels of ICAM-5 were found in the newborn MMP-2– or MMP-9–deficient mice (Fig. 4 A), supporting the finding of involvement of MMP-2 and -9 in ICAM-5 proteolytic processing.

Interestingly, the difference in ICAM-5 expression between the MMP-2– or MMP-9–deficient mice and the WT mice gradually disappeared during postnatal brain development (Fig. 4 A), which may partially be due to the decrease of MMP-2 enzymatic activity (Fig. 4 B) with the simultaneous increase of ICAM-5 expression during the later postnatal period. In contrast to ICAM-5, another important CAM, L1CAM, did not show changes in the expression levels in the MMP-2– or MMP-9–deficient mice as compared with the WT mice. Furthermore, L1CAM showed a gradual decrease in expression during the postnatal period (Fig. 4 A), indicating a shift of roles between the two molecules during brain maturation.

An earlier report on MMP-2–deficient mice has shown that MMP-9 activity is up-regulated (Esparza et al., 2004). Here, we found a similar phenomenon in the brains of adult MMP-2–deficient mice (Fig. 4 B). The expression of ICAM-5 in the MMP double-deficient mice was reduced during the early postnatal period (Fig. 4 A), which may be due to compensating effects of other proteases. Another possibility could be that protein synthesis is deficient in these mice because of developmental defects.

We found that the cytoskeletal anchorage of membrane-bound ICAM-5 was critical for controlling its proteolytic cleavage by MMPs. Disruption of actin filaments by cytochalasin D or latrunculin A, or deletion of the cytoplasmic tail of ICAM-5, significantly promoted its cleavage. Activation of the NRs resulted in dissociation of ICAM-5 from the actin cytoskeleton. The actin cytoskeleton determines the shape, motility, and stability of dendritic spines and provides the substrates for the Rho family small GTPases, which are the key regulators of actin polymerization and spine motility (Scott and Luo, 2001; Calabrese et al., 2006). The NRs and GluRs have been shown to promote

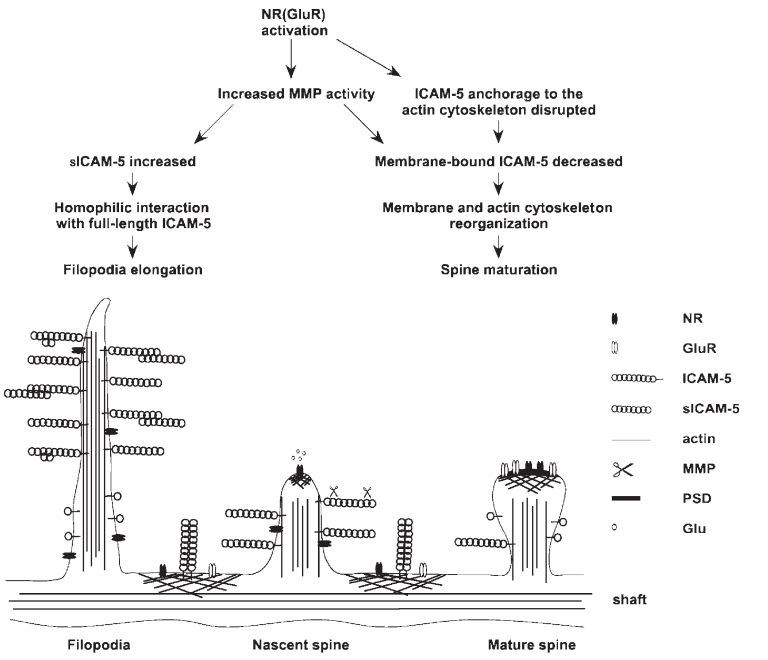

Figure 10. **Schematic model of ICAM-5 involvement in spine maturation and filopodia elongation through activation of glutamate receptors.** The activation of NRs or GluRs in neurons induces increased MMP-2 and -9 activities, which cleave the ectodomains of ICAM-5 from nascent spines, and results in dissociation of ICAM-5 from the actin cytoskeleton. The remaining CTF of ICAM-5 may compete and disrupt the anchorage of full-length ICAM-5 to the actin cytoskeleton, which further promotes its cleavage from spines by MMPs. Reduced membrane levels of ICAM-5 may facilitate local membrane and cytoskeleton reorganization, which induces the maturation of dendritic spines. Concomitantly, the sICAM-5 fragments produced by MMPs can bind in homophilic manner to the full-length ICAM-5 in the neighborhood filopodia and promote their elongation.

formation and stabilization of dendritic spines, respectively, by inhibiting the actin-based protrusive activity from the spine heads (Fischer et al., 2000) and increasing the turnover time of dynamic actin in spines (Star et al., 2002). Inhibition of actin motility caused spines to round up so that spine morphology became more stable and regular (Fischer et al., 2000). These facts indicate that the cytoplasmic part of ICAM-5 participates in the NR-dependent morphological change of spines by exerting a regulatory role on MMP-mediated ICAM-5 cleavage.

We have shown that ICAM-5 associates with the actin filaments via α-actinin and promotes neuritic outgrowth (Nyman-Huttunen et al., 2006). The NR subunit (NR2B) has been shown to interact with α-actinin (Wyszynski et al., 1997; Husi et al., 2000). α-Actinin has been implicated in the regulation of spine morphology (Nakagawa et al., 2004). Therefore, it is plausible that the NR may directly compete with ICAM-5 for interaction with actin filaments (Fig. 10).

The role of MMPs in the normal brain development is gradually becoming apparent (Dzwonek et al., 2004; Luo, 2005; Ethell and Ethell, 2007). However, little is known concerning the effects of MMPs on dendritic spine development, even though both their ECM and non-ECM substrates in the brain have been found to be important for spine formation and remodeling (Ethell and Pasquale, 2005). Recently, MMP-7 (Bilousova et al., 2006), MMP-9 (Meighan et al., 2006; Nagy et al., 2006), and MMP-24 (Monea et al., 2006) were shown to be involved in dendritic filopodia elongation or synaptic remodeling. Particularly, MMP-9–deficient mice show impaired LTP and behavioral impairments in hippocampus-dependent associative learning (Nagy et al., 2006), suggesting the potential importance of MMP on dendritic spine development.

Although mutant mice lacking individual MMPs have been generated (Itoh et al., 1997; Vu et al., 1998), no obvious defects in embryogenesis have been reported. In particular, MMP-2–deficient mice seemed to be healthy and fertile (Itoh et al., 1997), although they exhibited defects in bone metabolism (Inoue et al., 2006). We found that MMP-2–deficient mice seemed to have an increased number of cells in the cerebral cortex, especially in layers 2–3 (Fig. S4). Similar findings have been reported in the cerebellar cortex of MMP-9–deficient mice, which showed an abnormal accumulation of granular precursors in the external granular layer (Vaillant et al., 2003). Thus, our findings on MMP-2–deficient mice deserve more careful and detailed study in the future.

In summary, we have defined a physiological mechanism for the proteolytic processing of ICAM-5 by MMP-2 and -9, and the importance of its cleavage on regulation of dendritic spine development. Our results will help elucidate the functions of both MMPs and adhesion molecules on dendritic development, which is still poorly understood.

Materials and methods

Reagents and antibodies

AMPA, DNQX, gelatin, MK-801, NMDA, and poly-L-lysine were obtained from Sigma-Aldrich. Cytochalasin D, Latrunculin A, GM6001, GM6001 Neg. Ctrl, MMP-2/MMP-9 inhibitor II, and MMP-9 inhibitor I were obtained from Calbiochem. ProMMP-2 and -9 were obtained from Roche. CTT and $CTT_{W/A}$ peptides were gifts from E. Koivunen (Division of Biochemistry, University of Helsinki, Helsinki, Finland; Koivunen et al., 1999).

The pAb anti–ICAM-5cp against the cytoplasmic tail of mouse ICAM-5 was a gift from Y. Yoshihara (Brain Science Institute/Institute of Physical and Chemical Research, Wako City, Japan). The pAb 1000J and the mAb 127E, both against the ectodomain of rat ICAM-5, were gifts from P. Kilgannon (ICOS Corporation, Seattle, WA). The anti-L1CAM mAb, anti–MAP-2 mAb, and the anti-PSD95 mAb and pAb were obtained from Abcam. The anti-actin pAb was obtained from Sigma-Aldrich. The pAbs against MMP-2 and -9 were obtained from Santa Cruz Biotechnology, Inc., and Chemicon, respectively. A mAb negative control was also obtained from Chemicon. Peroxidase-conjugated anti-mouse, anti-rabbit, and anti-human pAbs were obtained from GE Healthcare. Alexa488-, Cy3-, or Cy5-conjugated anti-mouse and anti-rabbit pAbs and Cy3-conjugated phalloidin were obtained from Invitrogen.

Animals

MMP-2–, MMP-9–, and ICAM-5–deficient mice were generated by gene targeting (Itoh et al., 1997; Vu et al., 1998; Nakamura et al., 2001). All animals were backcrossed at least six generations into a homogenous C57BL/6 genetic background and were bred as homozygous lines. Mice deficient in both MMP-2 and -9 were obtained by intercrossing mice that were heterozygous for both mutations. All experiments were approved by and performed according to the guidelines of the local animal ethical committee.

Cell culture

Paju-Mock, Paju-ICAM-5-fl, and Paju-ICAM-5-ΔCP cell lines and hippocampal neurons were prepared as described earlier (Nyman-Huttunen et al., 2006). The CHO cell line stably expressing ICAM-5 D1- 4-Fc recombinant protein, a gift from J. Casasnovas (Universidad Autonoma, Madrid, Spain), was grown as recommended (Casasnovas et al., 1998).

Cell stimulation and sICAM-5 detection

During the 3-wk period of in vitro cultivation of hippocampal neurons, the culture media were replaced with HBSS with 1.8 mM $CaCl_2$ buffer for 16 h on days 3, 7, 14, and 21. The 14-DIV hippocampal neurons were treated for 16 h with 5 μM NMDA or AMPA, with or without a 2-h pretreatment with 20 μM MK-801 or DNQX, respectively, in HBSS/Ca^{2+} buffer. When MMP inhibitors were applied, 20–25 μM chemical inhibitors or 100 μM peptide inhibitors were used together with NMDA. Paju-ICAM-5-fl and Paju-ICAM-5-ΔCP cells were incubated in serum-free culture media for 18 h. Then, 1-ml aliquots of the conditioned culture media were concentrated 20-fold by Vivaspin centrifugal concentrators (Sartorius Ltd.), and the cells were stripped off. All samples were suspended in Laemmli sample buffer for Western blotting.

RNA interference

9-DIV rat hippocampal neurons were transfected with 50 nM predesigned siRNAs against rat MMP-2, MMP-9, or negative control siRNA (Ambion) using Lipofectamine RNAiMAX reagent (Invitrogen) for 48 h. The culture media were changed into HBSS/Ca^{2+} buffer for 16 h and then collected and concentrated for Western blotting.

Crude brain membrane preparations

Forebrains from the postnatal 1 d ($n = 4$), 1 wk ($n = 2$), and 10 wk ($n = 2$) MMP-deficient or WT mice were homogenized with buffer containing 0.32 M sucrose, 10 mM Hepes, pH 7.4, 2 mM EDTA, 50 mM NaF, 1 mM Na_2VO_4, and 1× protease cocktail inhibitors, using a glass-teflon homogenizer. The homogenates were then centrifuged at 1,000 *g*, and the supernatants were centrifuged at 50,000 rpm to separate the membrane fractions from the soluble fractions. The membrane fractions were suspended in lysis buffer (1% Triton X-100, 50 mM Hepes, pH 7.4, 2 mM EDTA, and protease/phosphatase inhibitors). For Western blotting, 20 μg of protein from each sample was suspended in Laemmli sample buffer.

Subcellular fractionations

14-DIV hippocampal neurons were either left untreated or treated with 20 μM NMDA for 60 min, and cells were then lysed in lysis buffer. Lysates were centrifuged at 5,000 rpm to get rid of the nuclear fractions, and the supernatants were further centrifuged at 100,000 rpm for 2 h at +2°C to separate the cytoskeletal fractions from the soluble fractions, and each sample was suspended in Laemmli sample buffer for Western blotting.

Recombinant protein purification

Recombinant human ICAM-5 D1-4-Fc and mouse ICAM-5 D1-9-Fc proteins were purified from cell culture supernatants by affinity chromatography with protein A–Sepharose and ÄKTAprime system (GE Healthcare).

In vitro cleavage and detection of recombinant ICAM-5-Fc protein
ProMMP-2 and -9 were activated with p-aminophenylmercuric acetate and trypsin, respectively, and 40 ng of activated enzymes was incubated with 2 μg ICAM-5 D1-9-Fc protein in 50 μl enzyme buffer (20 mM Hepes, 150 mM NaCl, 0.2 mM $CaCl_2$, 1 mM $MnCl_2$, and 1 μM $ZnCl_2$) at 37°C for 18 h. 5 μl of the enzyme-substrate mixtures were suspended in sample buffer.

Western blotting
Samples were separated by 4–12% SDS-PAGE (Invitrogen) and transferred to nitrocellulose membranes (Whatman GmbH). After blocking, membranes were incubated with anti–ICAM-5 pAb 1000J, anti–ICAM-5cp pAb, anti-L1CAM mAb, anti-actin pAb, or horseradish peroxidase–conjugated anti-human pAb, respectively, followed by peroxidase-conjugated secondary antibodies. Membranes were washed with TBS and 0.05% Tween 20 after each incubation and developed with an ECL kit (GE Healthcare). Band intensity was quantified by the software Tina 2.09c (Raytest).

Gelatinase zymography
20 μl of 60-fold–concentrated serum-free cell culture media or 50 μg of protein from brain membrane fractions was suspended in sample buffer and separated by 8% SDS−PAGE containing 0.2% gelatin. Gels were then washed with 2.5% Triton X-100 to remove SDS and incubated in substrate buffer (50 mM Tris, pH 8, and 5 mM $CaCl_2$) for 18 h at 37°C, followed by staining with 0.5% Coomassie blue.

Mass spectrometry
About 1 μg ICAM-5 D1-9-Fc fragments after the MMP-2 or -9 digestion were separated by 4–12% SDS-PAGE (Invitrogen), silver stained, and analyzed in the Protein Chemistry Unit of the Institute of Biotechnology, University of Helsinki. The bands of interest were cut out, reduced with dithiothreitol, alkylated with iodoacetamide, and "in-gel" digested with trypsin (Sequencing Grade Modified Trypsin; V5111; Promega). The recovered peptides were, after desalting using μ-C18 ZipTip (Millipore), subjected to MALDI-TOF mass spectrometric analysis. MALDI-TOF mass spectra for mass fingerprinting and MALDI-TOF/TOF mass spectra for identification by fragment ion analysis were obtained using an Ultraflex TOF/TOF instrument (Bruker-Daltonik GmbH). Protein identification with the generated data was performed using Mascot Peptide Mass Fingerprint and MS/MS Ion Search programs.

Flow cytometry
Paju-Mock, Paju-ICAM-5-fl, or Paju-ICAM-5-ΔCP cells were incubated with 5 μg/ml mAb TL-3 and then with Alexa488-conjugated anti-mouse pAb (Invitrogen). Cells were washed with PBS after each incubation. Samples were analyzed with FACScan and CellQuest software (Becton Dickinson).

Immunofluorescence microscopy
Hippocampal neurons were transfected with pEGFP-N1 plasmid using Lipofectamine 2000 reagent (Invitrogen) at 8–9 DIV and cultured until 12–17 DIV. For filopodia elongation assay, the 9-DIV neurons were treated twice with 10 μg/ml of recombinant ICAM-5 D1-4-Fc protein or control mIgG for 72 h. The 10–12-DIV neurons were then fixed with 4% paraformaldehyde and permeabilized with 0.1% Triton X-100. After blocking with 2% BSA in PBS, neurons were stained with pAb anti–ICAM-5cp plus Alexa488- or Cy3-conjugated anti-rabbit IgG, Cy3-conjugated phalloidin, anti-PSD95 mAb, or anti-MAP-2 mAb plus Cy5-conjugated anti-mouse IgG. The 17-DIV neurons were left untreated or treated with 5 μM NMDA with or without a 2-h pretreatment with 20 μM MK801 or MMP inhibitors in HBSS/Ca^{2+} buffer for 6 h. The neurons were fixed, permeabilized, and blocked afterward, and stained with mAb 127E plus Cy3-conjugated anti-mouse IgG and anti-PSD95 pAb plus Cy5-conjugated anti-rabbit IgG. The fluorescent images were taken with a confocal laser-scanning microscope under 63× magnification (TCS SP2 AOBS, HCX PL APO 63×O/1.4-0.6; Leica) using a charge-coupled device camera (Leica) and the LCSLite software. Four to five neurons per sample were randomly imaged for each experiment. At least three proximal dendritic segments (~60 μm per segment) were analyzed for each neuron. Dendritic filopodia (>2 μm long with pointy tip), thin spines (0.5–2.5 μm long with bulbous tip and <0.1 μm thick in neck), or mushroom-shaped spines (0.5–2.0 μm long and 0.3–0.6 μm wide in head) were quantified and presented as numbers per 100 μm dendritic length. For live imaging, 14-DIV EGFP-transfected neurons were treated with 20 μM NMDA in HBSS/Ca^{2+} buffer, with or without pretreatment with 20 μM MK801 for 1 h, in 5% CO_2/10% O_2 at 37°C, and monitored with an inverted fluorescent microscope under 60× magnification (IX-71; UPlanSApo 60×W/1.2; Olympus) using an electron multiplying charge-coupled device camera (DV885; Andor Technology) and the TillVision software (Till Photonics GmbH). Images were processed with Photoshop and ImagePro plus. Pearson's coefficients were used for colocalization analysis.

Histology
Brains from 8-wk-old mice were fixed with 4% paraformaldehyde in PBS and embedded in paraffin wax. Coronal paraffin sections 10 μm thick were cut and mounted on glass slides. Brain sections were stained with cresyl violet and visualized with a light microscope (IX71; Olympus). Images were processed with Photoshop (Adobe).

Statistical analysis
t test was used to compare different groups of data.

Online supplemental material
Fig. S1 shows that NMDA increases the expression and activities of MMP-2 and -9. Fig. S2 shows peptide mass mapping of MMP-cleaved ICAM-5-Fc proteins. Fig. S3 shows flow cytometry analysis of transfected Paju cell lines. Fig. S4 shows abnormal cortical and hippocampal development in MMP-2–deficient mice. Online supplemental material is available at http://www.jcb.org/cgi/content/full/jcb.200612097/DC1.

We thank Dr. Yoshihiro Yoshihara for providing the anti–ICAM-5cp pAb; Dr. Patrick Kilgannon for rat ICAM-5 mAbs and pAb 1000J; Dr. Erkki Koivunen for MMP-inhibitory peptides; Dr. Jose Casasnovas for CHO cell lines; Dr. Nisse Kalkkinen for peptide mass mapping; Seija Lehto, Leena Kuoppasalmi, Outi Nikkilä, Erja Huttu, and Maria Aatonen for technical assistance; and Yvonne Heinilä for secretarial help.

This study was supported by the Sigrid Jusélius Foundation, the Academy of Finland, the Finnish Cultural Foundation, the Magnus Ehrnrooth Foundation, the Finnish Cancer Society, the Liv och Hälsa Foundation, and the Institute for the Promotion of Innovation through Science and Technology in Flanders (IWT-Vlaanderen).

Submitted: 18 December 2006
Accepted: 13 July 2007

References

Ayoub, A.E., T.Q. Cai, R.A. Kaplan, and J. Luo. 2005. Developmental expression of matrix metalloproteinases 2 and 9 and their potential role in the histogenesis of the cerebellar cortex. *J. Comp. Neurol.* 481:403–415.

Benson, D.L., Y. Yoshihara, and K. Mori. 1998. Polarized distribution and cell type-specific localization of telencephalin, an intercellular adhesion molecule. *J. Neurosci. Res.* 52:43–53.

Bilousova, T.V., D.A. Rusakov, D.W. Ethell, and I.M. Ethell. 2006. Matrix metalloproteinase-7 disrupts dendritic spines in hippocampal neurons through NMDA receptor activation. *J. Neurochem.* 97:44–56.

Borusiak, P., P. Gerner, C. Brandt, P. Kilgannon, and P. Rieckmann. 2005. Soluble telencephalin in the serum of children after febrile seizures. *J. Neurol.* 252:493–494.

Calabrese, B., M.S. Wilson, and S. Halpain. 2006. Development and regulation of dendritic spine synapses. *Physiology (Bethesda).* 21:38–47.

Casasnovas, J.M., T. Stehle, J.H. Liu, J.H. Wang, and T.A. Springer. 1998. A dimeric crystal structure for the N-terminal two domains of intercellular adhesion molecule-1. *Proc. Natl. Acad. Sci. USA.* 95:4134–4139.

Chakraborti, S., M. Mandal, S. Das, A. Mandal, and T. Chakraborti. 2003. Regulation of matrix metalloproteinases: an overview. *Mol. Cell. Biochem.* 253:269–285.

Dityatev, A., G. Dityateva, V. Sytnyk, M. Delling, N. Toni, I. Nikonenko, D. Muller, and M. Schachner. 2004. Polysialylated neural cell adhesion molecule promotes remodeling and formation of hippocampal synapses. *J. Neurosci.* 24:9372–9382.

Dzwonek, J., M. Rylski, and L. Kaczmarek. 2004. Matrix metalloproteinases and their endogenous inhibitors in neuronal physiology of the adult brain. *FEBS Lett.* 567:129–135.

Esparza, J., M. Kruse, J. Lee, M. Michaud, and J.A. Madri. 2004. MMP-2 null mice exhibit an early onset and severe experimental autoimmune encephalomyelitis due to an increase in MMP-9 expression and activity. *FASEB J.* 18:1682–1691.

Ethell, I.M., and E.B. Pasquale. 2005. Molecular mechanisms of dendritic spine development and remodeling. *Prog. Neurobiol.* 75:161–205.

Ethell, I.M., and D.W. Ethell. 2007. Matrix metalloproteinases in brain development and remodeling: synaptic functions and targets. *J. Neurosci. Res.* 10.1002/jnr.21273.

Ethell, I.M., F. Irie, M.S. Kalo, J.R. Couchman, E.B. Pasquale, and Y. Yamaguchi. 2001. EphB/syndecan-2 signaling in dendritic spine morphogenesis. *Neuron.* 31:1001–1013.

Fischer, M., S. Kaech, U. Wagner, H. Brinkhaus, and A. Matus. 2000. Glutamate receptors regulate actin-based plasticity in dendritic spines. *Nat. Neurosci.* 3:887–894.

Gahmberg, C.G., L. Valmu, S. Fagerholm, P. Kotovuori, E. Ihanus, L. Tian, and T. Pessa-Morikawa. 1998. Leukocyte integrins and inflammation. *Cell. Mol. Life Sci.* 54:549–555.

Gerrow , K., and A. El-Husseini. 2006. Cell adhesion molecules at the synapse. *Front. Biosci.* 11:2400–2419.

Guo, H., N. Tong, T. Turner, L.G. Epstein, M.P. McDermott, P. Kilgannon, and H.A. Gelbard. 2000. Release of the neuronal glycoprotein ICAM-5 in serum after hypoxic-ischemic injury. *Ann. Neurol.* 48:590–602.

Hering, H., and M. Sheng. 2001. Dendritic spines: structure, dynamics and regulation. *Nat. Rev. Neurosci.* 2:880–888.

Husi, H., M.A. Ward, J.S. Choudhary, W.P. Blackstock, and S.G. Grant. 2000. Proteomic analysis of NMDA receptor-adhesion protein signaling complexes. *Nat. Neurosci.* 3:661–669.

Inoue, K., Y. Mikuni-Takagaki, K. Oikawa, T. Itoh, M. Inada, T. Noguchi, J.S. Park, T. Onodera, S.M. Krane, M. Noda, and S. Itohara. 2006. A crucial role for matrix metalloproteinase 2 in osteocytic canalicular formation and bone metabolism. *J. Biol. Chem.* 281:33814–33824.

Itoh, T., T. Ikeda, H. Gomi, S. Nakao, T. Suzuki, and S. Itohara. 1997. Unaltered secretion of beta-amyloid precursor protein in gelatinase A (matrix metalloproteinase 2)-deficient mice. *J. Biol. Chem.* 272:22389–22392.

Kasai, H., M. Matsuzaki, J. Noguchi, N. Yasumatsu, and H. Nakahara. 2003. Structure-stability-function relationships of dendritic spines. *Trends Neurosci.* 26:360–368.

Koivunen, E., W. Arap, H. Valtanen, A. Rainisalo, O.P. Medina, P. Heikkila, C. Kantor, C.G. Gahmberg, T. Salo, Y.T. Konttinen, et al. 1999. Tumor targeting with a selective gelatinase inhibitor. *Nat. Biotechnol.* 17:768–774.

Lindsberg, P.J., J. Launes, L. Tian, H. Valimaa, V. Subramanian, J. Siren, L. Hokkanen, T. Hyypia, O. Carpen, and C.G. Gahmberg. 2002. Release of soluble ICAM-5, a neuronal adhesion molecule, in acute encephalitis. *Neurology.* 58:446–451.

Liu, W.S., C. Pesold, M.A. Rodriguez, G. Carboni, J. Auta, P. Lacor, J. Larson, B.G. Condie, A. Guidotti, and E. Costa. 2001. Down-regulation of dendritic spine and glutamic acid decarboxylase 67 expressions in the reelin haploinsufficient heterozygous reeler mouse. *Proc. Natl. Acad. Sci. USA.* 98:3477–3482.

Luo, J. 2005. The role of matrix metalloproteinases in the morphogenesis of the cerebellar cortex. *Cerebellum.* 4:239–245.

Malemud, C.J. 2006. Matrix metalloproteinases (MMPs) in health and disease: an overview. *Front. Biosci.* 11:1696–1701.

Matsuno, H., S. Okabe, M. Mishina, T. Yanagida, K. Mori, and Y. Yoshihara. 2006. Telencephalin slows spine maturation. *J. Neurosci.* 26:1776–1786.

Matsuzaki, M., N. Honkura, G.C. Ellis-Davies, and H. Kasai. 2004. Structural basis of long-term potentiation in single dendritic spines. *Nature.* 429:761–766.

Matus, A. 2000. Actin-based plasticity in dendritic spines. *Science.* 290:754–758.

Meighan, S.E., P.C. Meighan, P. Choudhury, C.J. Davis, M.L. Olson, P.A. Zornes, J.W. Wright, and J.W. Harding. 2006. Effects of extracellular matrix-degrading proteases matrix metalloproteinases 3 and 9 on spatial learning and synaptic plasticity. *J. Neurochem.* 96:1227–1241.

Mitsui, S., M. Saito, K. Hayashi, K. Mori, and Y. Yoshihara. 2005. A novel phenylalanine-based targeting signal directs telencephalin to neuronal dendrites. *J. Neurosci.* 25:1122–1131.

Monea, S., B.A. Jordan, S. Srivastava, S. DeSouza, and E.B. Ziff. 2006. Membrane localization of membrane type 5 matrix metalloproteinase by AMPA receptor binding protein and cleavage of cadherins. *J. Neurosci.* 26:2300–2312.

Nagy, V., O. Bozdagi, A. Matynia, M. Balcerzyk, P. Okulski, J. Dzwonek, R.M. Costa, A.J. Silva, L. Kaczmarek, and G.W. Huntley. 2006. Matrix metalloproteinase-9 is required for hippocampal late-phase long-term potentiation and memory. *J. Neurosci.* 26:1923–1934.

Nakagawa, T., J.A. Engler, and M. Sheng. 2004. The dynamic turnover and functional roles of alpha-actinin in dendritic spines. *Neuropharmacology.* 47:734–745.

Nakamura, K., T. Manabe, M. Watanabe, T. Mamiya, R. Ichikawa, Y. Kiyama, M. Sanbo, T. Yagi, Y. Inoue, T. Nabeshima, et al. 2001. Enhancement of hippocampal LTP, reference memory and sensorimotor gating in mutant mice lacking a telencephalon-specific cell adhesion molecule. *Eur. J. Neurosci.* 13:179–189.

Nyman-Huttunen, H., L. Tian, L. Ning, and C.G. Gahmberg. 2006. α-Actinin-dependent cytoskeletal anchorage is important for ICAM-5-mediated neuritic outgrowth. *J. Cell Sci.* 119:3057–3066.

Oertner, T.G., and A. Matus. 2005. Calcium regulation of actin dynamics in dendritic spines. *Cell Calcium.* 37:477–482.

Oray, S., A. Majewska, and M. Sur. 2004. Dendritic spine dynamics are regulated by monocular deprivation and extracellular matrix degradation. *Neuron.* 44:1021–1030.

Portera-Cailliau, C., D.T. Pan, and R. Yuste. 2003. Activity-regulated dynamic behavior of early dendritic protrusions: evidence for different types of dendritic filopodia. *J. Neurosci.* 23:7129–7142.

Scott, E.K., and L. Luo. 2001. How do dendrites take their shape? *Nat. Neurosci.* 4:359–365.

Shi, Y., and I.M. Ethell. 2006. Integrins control dendritic spine plasticity in hippocampal neurons through NMDA receptor and Ca^{2+}/calmodulin-dependent protein kinase II-mediated actin reorganization. *J. Neurosci.* 26:1813–1822.

Star, E.N., D.J. Kwiatkowski, and V.N. Murthy. 2002. Rapid turnover of actin in dendritic spines and its regulation by activity. *Nat. Neurosci.* 5:239–246.

Szklarczyk, A., J. Lapinska, M. Rylski, R.D. McKay, and L. Kaczmarek. 2002. Matrix metalloproteinase-9 undergoes expression and activation during dendritic remodeling in adult hippocampus. *J. Neurosci.* 22:920–930.

Tada, T., and M. Sheng. 2006. Molecular mechanisms of dendritic spine morphogenesis. *Curr. Opin. Neurobiol.* 16:95–101.

Tian, L., H. Nyman, P. Kilgannon, Y. Yoshihara, K. Mori, L.C. Andersson, S. Kaukinen, H. Rauvala, W.M. Gallatin, and C.G. Gahmberg. 2000. Intercellular adhesion molecule-5 induces dendritic outgrowth by homophilic adhesion. *J. Cell Biol.* 150:243–252.

Togashi, H., K. Abe, A. Mizoguchi, K. Takaoka, O. Chisaka, and M. Takeichi. 2002. Cadherin regulates dendritic spine morphogenesis. *Neuron.* 35:77–89.

Vaillant, C., C. Meissirel, M. Mutin, M.F. Belin, L.R. Lund, and N. Thomasset. 2003. MMP-9 deficiency affects axonal outgrowth, migration, and apoptosis in the developing cerebellum. *Mol. Cell. Neurosci.* 24:395–408.

Vu, T.H., J.M. Shipley, G. Bergers, J.E. Berger, J.A. Helms, D. Hanahan, S.D. Shapiro, R.M. Senior, and Z. Werb. 1998. MMP-9/gelatinase B is a key regulator of growth plate angiogenesis and apoptosis of hypertrophic chondrocytes. *Cell.* 93:411–422.

Washbourne, P., A. Dityatev, P. Scheiffele, T. Biederer, J.A. Weiner, K.S. Christopherson, and A. El-Husseini. 2004. Cell adhesion molecules in synapse formation. *J. Neurosci.* 24:9244–9249.

Wyszynski, M., J. Lin, A. Rao, E. Nigh, A.H. Beggs, A.M. Craig, and M. Sheng. 1997. Competitive binding of alpha-actinin and calmodulin to the NMDA receptor. *Nature.* 385:439–442.

Yoshihara, Y., S. Oka, Y. Nemoto, Y. Watanabe, S. Nagata, H. Kagamiyama, and K. Mori. 1994. An ICAM-related neuronal glycoprotein, telencephalin, with brain segment-specific expression. *Neuron.* 12:541–553.

Yuste, R., and T. Bonhoeffer. 2004. Genesis of dendritic spines: insights from ultrastructural and imaging studies. *Nat. Rev. Neurosci.* 5:24–34.